

Diffractive production of $\pi^- \pi^- \pi^+$ in 200-GeV/c $\pi^- N$ interactions

R. W. Joyner, C. C. Chang, T. C. Davis, R. N. Diamond, K. J. Johnson,
S. Mikocki, and J. A. Poirier

University of Notre Dame, Notre Dame, Indiana 46556

T. Y. Chen, E. W. Jenkins, K. W. Lai, Y. C. Lin, and A. E. Pifer

University of Arizona, Tucson, Arizona 85721

H. C. Fenker and D. R. Green

Fermi National Accelerator Laboratory, Batavia, Illinois 60510

J. R. Albright, J. H. Goldman, S. L. Hagopian, and J. E. Lannutti

Florida State University, Tallahassee, Florida 32306

A. Napier and J. Schneps

Tufts University, Medford, Massachusetts 02155

J. M. Marraffino, J. W. Waters, and M. S. Webster

Vanderbilt University, Nashville, Tennessee 37235

J. R. Ficenec and W. P. Trower

Virginia Polytechnic Institute and State University, Blacksburg, Virginia 24061

(Received 16 November 1987; revised manuscript received 10 November 1988)

This paper analyzes $\pi^- N \rightarrow \pi^- \pi^- \pi^+ N$ events from Fermilab experiment E-580, using 200-GeV/c particles on a segmented target of plastic scintillator. Starting with 48 657 triggers, data-quality cuts and a cut on missing mass squared of $M^2 < 16 \text{ GeV}^2$ lead to a final sample of 7205 events. The x_F distribution of the 3π system shows almost all events in a sharp peak at $x_F = 1$, suggesting the presence of beam diffraction into three pions. The overall t' distribution is fit to the sum of three exponential terms corresponding to coherent diffraction from carbon nuclei, diffraction from individual nucleons, and background. Cross sections per nucleon and exponential slopes are reported for each of the three components as a function of 3π effective mass. The cross section for diffraction from the nucleons in the target is $0.34 \pm 0.04 \text{ mb/nucleon}$. The cross section for coherent diffraction from carbon is $1.08 \pm 0.12 \text{ mb/nucleus}$. The exponential slope for diffraction is observed to decrease with increasing 3π effective mass. The fraction of coherent carbon diffraction in the total cross section is observed to decrease with increasing 3π effective mass. In the $\pi^- \pi^+$ effective-mass spectrum the $\rho^0(770)$ and $f^0(1270)$ are observed and their cross sections per nucleon are calculated. In the $\pi^- \pi^- \pi^+$ effective-mass spectrum the A_1^- / A_2^- and A_3^- enhancements are observed and a cross section for the A_3^- is calculated.

The diffractive production of $\pi^- \pi^- \pi^+$ has been widely studied at a variety of energies,¹⁻¹⁴ but rarely at the high energy of 200 GeV (Refs. 15-17). This paper presents results on the diffractive dissociation of a 200-GeV/c π^- beam into $\pi^- \pi^- \pi^+$.

Experiment E-580 at Fermilab was carried out in the M6W beam line using the Fermilab multiparticle spectrometer (MPS) (Ref. 18). The target consisted of 13 cm of plastic ($\text{C}_1\text{H}_{1.1}$) scintillator in 20 segments, providing longitudinal vertex information. A spectrometer dipole magnet imparted a 697-MeV/c transverse-momentum kick. A proportional-wire-chamber (PWC) system of 10 000 wires, plus 24 planes of magnetostrictive spark chamber, provided tracking information. References 18 and 19 contain additional experimental details.

The data in this analysis are from 48 657 events in

which the segmented target registered a multiplicity increase, and a majority of the PWC planes used in the fast trigger logic registered three tracks. The ensuing quality cuts, which include requiring two negative tracks and one positive track, ensuring that tracks are unique, requiring that all tracks project to within six σ of the event vertex, and requiring the total energy of the final state be less than 250 GeV, bring the sample down to 18 933 events. The loose cut at 250 GeV was made to eliminate a very few events with track-reconstruction problems, for example, elastic scatters which give reconstructed tracks of unphysically high momenta. No attempt at particle identification has been made; contamination from K^+ , K^- , p , or \bar{p} has been assumed to be negligibly small.

Figure 1 shows the distribution of missing-mass squared, assuming a proton mass for the target. The dis-

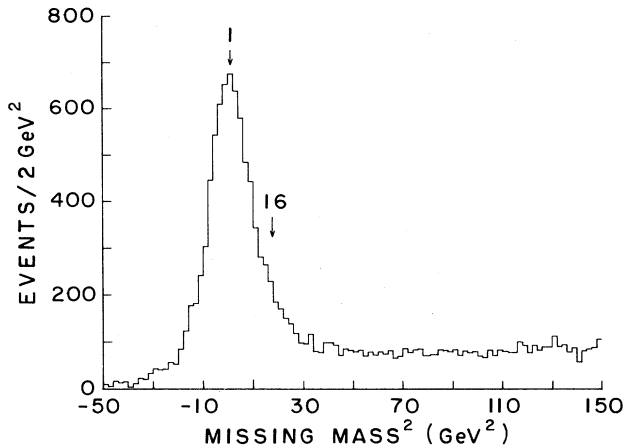


FIG. 1. Missing-mass squared in 2-GeV² bins; the target is assumed to have the mass of a proton. There are 18 933 events after quality cuts. Arrow 1 indicates the mass squared of a proton; 16 marks the data cut at 16 GeV².

tribution peaks at 1 GeV², the mass squared of a proton. A cut is made at 16 GeV² to remove unseen neutrals and to conform with the cut in the previously published $K_S^0 K_S^0 \pi^-$ and $K_S^0 K_S^0 \pi^- \pi^- \pi^+$ samples.^{19,20} After this cut, 7563 events remain. It is estimated that double diffraction is present in $\sim 20\%$ of the events.²¹

A fiducial-volume cut around the veto counter placed downstream of the spectrometer magnet at the location of the deflected beam brings the final sample to 7205 events. All further calculations in this paper are made with the final sample of 7205 events which remain after the above-mentioned cuts, including the missing-mass squared cut of 16 GeV², and the fiducial-volume cut around the veto counter.

These 7205 events were passed through a geometrical model of the MPS, and rotated 100 times each about the beam axis to determine an event-by-event weight to be used later for weighting each event. "Weighted events" are the experimentally observed events each multiplied by its individually calculated weight to correct it to the real number that would have been observed in an experiment with 100% geometrical detection efficiency. The overall geometrical acceptance was 0.730 ± 0.058 , and did not vary strongly with the mass of the event.

The sensitivity was calculated as follows. The effective beam was 22.9×10^6 incident pions. The density thickness of the target was 15.60 ± 0.16 g/cm². The trigger efficiency, calculated by using the measured efficiencies of the trigger PWC's, was 0.365 ± 0.029 . Reconstruction efficiency, calculated by passing actual events through a model of the MPS and then duplicating the software reconstruction, was 0.784 ± 0.029 . The efficiency of a fiducial cut to eliminate events in the vicinity of the beam veto counter was calculated to be 0.910 ± 0.003 .

For the carbon coherent diffraction cross section our experiment has a sensitivity of 4.27 ± 0.38 weighted events per microbarn of carbon-nucleus cross section. This sensitivity number incorporates the exact target composition which was comprised of small quantities of aluminum foil

and polyethylene tape besides the plastic scintillator. This number includes a 4.3% correction for the contribution from the coherent diffraction of the aluminum foil in the target.

For calculations involving noncarbon diffraction we calculate a sensitivity number of 31.5 ± 4.0 weighted events per microbarn cross section for each nucleon in the target. For this calculation we have used an effective number of nucleons per nucleus¹⁵ of A^α where A is the atomic weight and α we determine experimentally to be 0.74 ± 0.04 . These sensitivities have been calculated directly from the measured parameters of the experiment and have not been normalized in any way. The method of calculating the geometrical weight for each observed event is described above.

The overall $\pi^+ \pi^- \pi^-$ cross section for the 7205 events is thus 342 ± 43 $\mu\text{b}/\text{nucleon}$. We compare this cross section with the diffractive cross section in the E-580 $K_S^0 K_S^0 \pi^-$ reaction of 3.4 ± 1.1 $\mu\text{b}/\text{nucleon}$,¹⁹ and the $K_S^0 K_S^0 \pi^- \pi^- \pi^+$ reaction of 1.6 ± 0.7 $\mu\text{b}/\text{nucleon}$.²⁰ These numbers are consistent with expectations that heavy flavor (in this case strangeness) production leads to a large drop in cross section (by 2 orders of magnitude).

In order to determine the quality of the sample, the distribution of x_F (where $x_F = 2P_L^{c.m.}/\sqrt{s}$, $P_L^{c.m.}$ is the component of the momentum of the 3π system parallel to the beam, and \sqrt{s} is the center-of-mass energy) of the 3π system is shown in Fig. 2. It is seen that the sample consists almost totally of events in the peak at $x_F = +1$, indicating the predominance of events in which the incident π^- dissociates into 3π with minimal loss of forward momentum. This is evidence that, aside from double diffraction, this is a very clean sample.

Figure 3 shows the t' distribution for the entire sample, using weighted events, where

$$t' = 2P_{\text{bm}} P_{3\pi} (1 - \cos\theta),$$

where P_{bm} is total beam momentum, $P_{3\pi}$ is the total

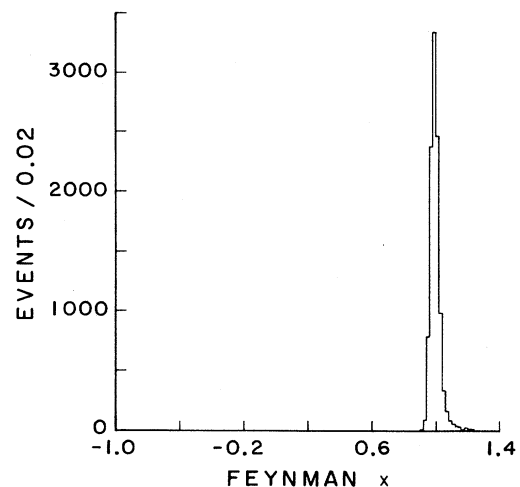


FIG. 2. Feynman x of the 3π system for the final sample of 7205 events.

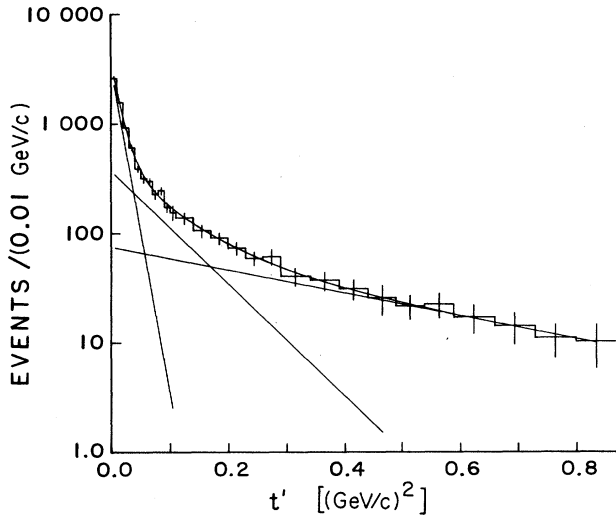


FIG. 3. Momentum transfer t' for the full final sample, with each event weighted for acceptance. The bins are $0.01 (\text{GeV}/c)^2$ wide. The curves are explained in the text. The vertical scale is logarithmic.

momentum of the 3π system, and θ is the angle between the incident beam and the outgoing 3π system. A fit to the distribution in the form

$$N(t') = A_1 \exp(-b_1 t') + A_2 \exp(-b_2 t') + A_3 \exp(-b_3 t')$$

was done, where the first exponential represents coherent diffraction from carbon nuclei, the second represents diffraction from individual nucleons, and the third signifies the background.²² A fit to this distribution gives $b_1 = 67.8 \pm 4.4 (\text{GeV}/c)^{-2}$, $b_2 = 11.8 \pm 3.4 (\text{GeV}/c)^{-2}$, and $b_3 = 2.4 \pm 0.9 (\text{GeV}/c)^{-2}$ with a χ^2 of 12 for 21 degrees of freedom. The fact that the t' distribution fits such a functional form is additional evidence that this is indeed a diffractive sample.

The 7205 events were subdivided according to 3π effective mass, and the t' distribution in each region fit separately. The regions were (in units of GeV/c^2): (1) $0.00 < M(3\pi) < 1.10$ (low-mass region), (2) $1.10 < M(3\pi) < 1.40$ (A_1/A_2 region), (3) $1.40 < M(3\pi) < 1.55$ (intermediate nonresonance region), (4) $1.55 < M(3\pi) < 1.80$ (A_3 region), and (5) $1.80 < M(3\pi)$ (high-mass region). The number of events, the fit parameters, and the cross

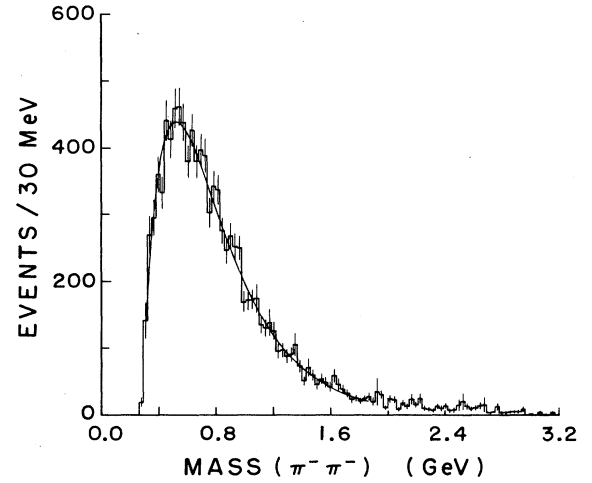


FIG. 4. Effective mass of $\pi^- \pi^- \pi^-$ combinations for the final sample, with each event weighted for acceptance. The bins are 30 MeV wide. The curve is a fit to the data as explained in the text.

sections are given in Table I by region and type of event. The last two columns are in units of microbarns per nucleon for all the data for purposes of comparison with hydrogen data.

It may be noted that the single-nucleon slope b_2 shows a general decreasing trend with rising 3π mass, which has been observed elsewhere.^{2,3,9,23} The coherent carbon slope b_1 displays ragged behavior, and shows rough agreement with Ref. 16.

Also of note is the ratio of $\sigma(\text{carbon})/\sigma(\text{nucleon})$, which decreases with rising 3π mass. At low mass this ratio is 14 which decreases to 5 at high mass. This indicates that coherent diffraction tends to favor low-mass states, and decreases in proportion to single-nucleon diffraction as the mass rises. This has been observed previously.¹¹

Of particular note is the overall cross section per nucleus in coherent carbon diffraction of 1.09 ± 0.13 mb/nucleus. This is to be compared with a value of 1.80 ± 0.32 mb/nucleus obtained at 200 GeV/c by Zielinski *et al.* in Ref. 16 for a mass range from 0.80 to 1.50 GeV/c^2 . Assuming an A^α dependence of the cross section, we find α to be 0.74 ± 0.04 . This value is consistent with the value of $0.75^{+0.09}_{-0.14}$ quoted in Ref. 15.

TABLE I. For several regions of 3π effective mass, exponential slopes b_1 (carbon), b_2 (nucleon), and b_3 (background) are listed. The cross sections are given for carbon diffraction (per carbon nucleus), nucleon diffraction (per nucleon), and the total of the three separate contributions (per nucleon). The χ^2 and the number of degrees of freedom for each fit are also given. The all $M(3\pi)$ row was obtained from a separate fit to all the data.

	b_1 [[GeV/c] ⁻²]	b_2 [[GeV/c] ⁻²]	b_3 [[GeV/c] ⁻²]	χ^2/N_{DF}	$\sigma(\text{carbon})$ ($\mu\text{b}/\text{nucleus}$)	$\sigma(\text{nucleon})$ ($\mu\text{b}/\text{nucleon}$)	$\sigma(\text{tot})$ ($\mu\text{b}/\text{nucleon}$)
$M3\pi < 1.10$	69±9	13±5	0.9±3	6/21	244±80	17±4	56±7
$1.10 < M3\pi < 1.40$	64±6	11±6	3.0±2.1	15/23	473±63	31±16	121±15
$1.40 < M3\pi < 1.55$	71±10	9±3	0.5±2.9	17/21	117±17	14±4	35±4
$1.55 < M3\pi < 1.80$	83±16	12±7	2.2±2.0	8/21	119±26	14±8	50±6
$1.80 < M3\pi$	51±4	4.3±0.4	0.1±0.3	9/21	192±104	39±6	79±10
All $M3\pi$	68±4	12±3	2.4±0.9	12/21	1084±123	98±10	342±43

Figure 4 shows the effective-mass distribution using weighted events for all $\pi^-\pi^+$ combinations; it is featureless. A fit to the form

$$N = (M - M_T)^\alpha \exp(-\beta M - \gamma M^2),$$

where $M_T = 2M_\pi$, gives a χ^2/N_{DF} of 56.2/49; a 23% probability.

The effective mass of all $\pi^-\pi^+$ combinations, using weighted events, is shown in Fig. 5. The most evident feature is the large peak around 0.77 GeV/c², corresponding to the $\rho^0(770)$. A second enhancement is seen around 1.27 GeV/c², corresponding to the $f^0(1270)$. A fit to the distribution, using the same functional form used above for the $\pi^-\pi^+$ as background, plus two Breit-Wigner resonance forms, gives $M(\rho^0) = 773 \pm 1$ MeV/c², $\Gamma(\rho^0) = 169 \pm 49$ MeV/c², $M(f^0) = 1268 \pm 9$ MeV/c², $\Gamma(f^0) = 178 \pm 27$ MeV/c², with a χ^2/N_{DF} of 57.1/43. These values are consistent with established average values.²⁴

It is observed that the percentages of ρ^0 comprise $(81.3 \pm 6.4)\%$, and f^0 comprise $(10.4 \pm 1.1)\%$ of the total sample, consistent with those found in Ref. 25. The cross sections per nucleon of these resonances are calculated to be

$$\sigma(\rho^0 \rightarrow \pi^-\pi^+) = 270 \pm 40 \mu\text{b/nucleon},$$

$$\sigma(f^0 \rightarrow \pi^-\pi^+) = 35 \pm 6 \mu\text{b/nucleon}.$$

Figure 6 shows the $\pi^-\pi^-\pi^+$ effective mass spectrum. Enhancements corresponding to the A_1^-/A_2^- and A_3^- are clearly seen. Because of the small size of the sample a partial-wave analysis was not performed and we were unable to obtain the relative sizes of the A_1^- and A_2^- contributions. However, a cut in the $\pi^-\pi^+$ effective mass corresponding to the $f^0(1270)$, $1.14 < M(\pi^-\pi^+) < 1.36$ GeV/c², has been made, and the results are shown in Fig.

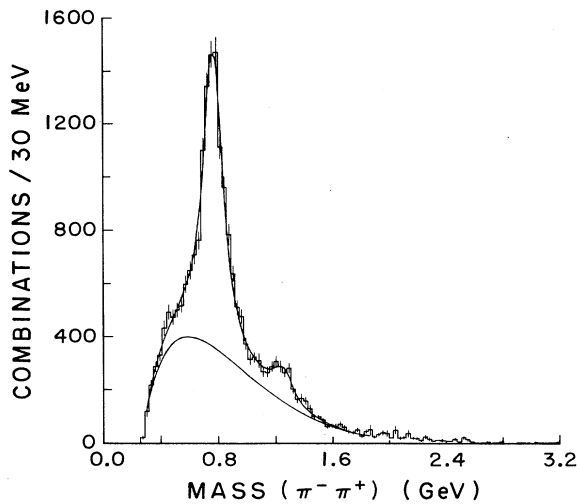


FIG. 5. Effective mass of $\pi^-\pi^+$ combinations for the final sample, with each event weighted for acceptance. The bins are 30 MeV wide. There are two entries per event. The curves shown are explained in the text.

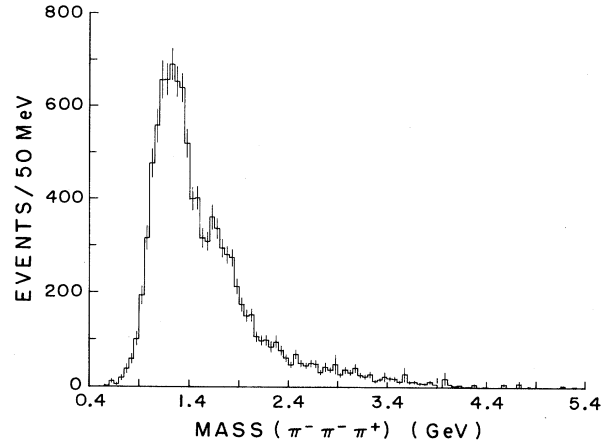


FIG. 6. Effective mass of the $\pi^-\pi^-\pi^+$ system for the final sample, with each event weighted for acceptance. The bins are 50 MeV wide.

7. A fit was performed to the same background form as was used for $M(\pi^-\pi^+)$, with M_T allowed to vary, plus a Breit-Wigner resonance form. The results give $M(A_3^-) = 1688 \pm 17$ MeV/c², $\Gamma(A_3^-) = 293 \pm 39$ MeV/c², with a χ^2/N_{DF} of 24/25. The numbers are consistent with established values.²⁴

The cross section per nucleon of the A_3^- has been calculated, adding a 20% systematic error to the number of A_3^- events observed due to the fact that the A_3^- is not in reality a pure Breit-Wigner resonance.^{2,8,9} The cross section is

$$\sigma(A_3^- \rightarrow f^0 \pi^- \rightarrow \pi^+ \pi^- \pi^-)$$

$$= 15.9 \pm 2.4 \pm 3.7 \mu\text{b/nucleon},$$

where the first error is statistical and the second is systematic.

In summary, the diffractive dissociation of π^- into $\pi^-\pi^-\pi^+$ is observed at 200 GeV/c, with a total cross section for events with missing-mass squared $M^2 < 16$ (GeV)² of $342 \pm 43 \mu\text{b/nucleon}$. The t' distribution of the events is fit by a sum of three exponentials representing both coherent carbon diffraction and single-nucleon diffraction and the background. The exponential slope of

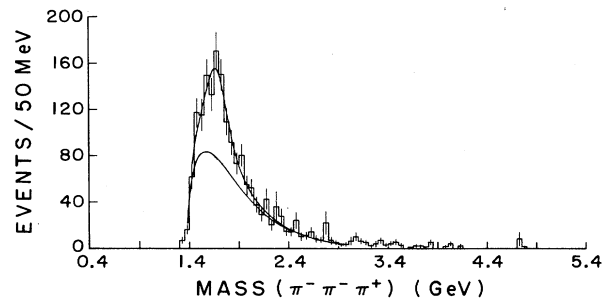


FIG. 7. The distribution of $\pi^-\pi^-\pi^+$ effective mass, with one $\pi^-\pi^+$ combination having effective mass $1.14 < M(\pi^-\pi^+) < 1.36$ GeV, and each event weighted for acceptance. The bins are 50 MeV wide. The curves shown are explained in the text.

the fit to the t' distribution is observed to decrease with rising 3π mass. The proportion of coherent carbon to single-nucleon events is observed to decrease with rising 3π mass. An A^α dependence of the cross section is found to have $\alpha=0.74\pm 0.04$. The $\rho^0(770)$ and $f^0(1270)$ are seen in the $\pi^-\pi^+$ effective mass spectrum, with cross sections of $270\pm 40 \mu\text{b/nucleon}$ and $35\pm 6 \mu\text{b/nucleon}$, respectively. The A_1^-/A_2^- and A_3^- enhancements are observed in the effective mass spectrum, and the coherent cross section for producing the A_3^- which decays to this final

state is found to be

$$\sigma(A_3^-) = 15.9 \pm 2.4(\text{stat}) \pm 3.7(\text{syst}) \mu\text{b/nucleon} .$$

We thank the Fermilab staff, especially S. Hansen and R. Cantel, for their valuable help during the experiment. Z. Ma provided helpful support. This work was supported by the Department of Energy (Arizona, Fermilab, Florida State, and Tufts) and the National Science Foundation (Arizona, Notre Dame, Vanderbilt, and Virginia Tech).

¹G. Ascoli *et al.*, Phys. Rev. D **7**, 669 (1973).

²Yu. M. Antipov *et al.*, Nucl. Phys. **B63**, 141 (1973).

³Yu. M. Antipov *et al.*, Nucl. Phys. **B63**, 153 (1973).

⁴J. Pernegr *et al.*, Nucl. Phys. **B134**, 436 (1978).

⁵J. A. Gaidos and W. L. Yen, Phys. Rev. D **19**, 22 (1979).

⁶D. Brick *et al.*, Phys. Rev. D **21**, 1726 (1980).

⁷R. Aaron and R. S. Longacre, Phys. Rev. D **24**, 1207 (1981).

⁸V. Chabaud *et al.*, Nucl. Phys. **B178**, 401 (1981).

⁹C. Daum *et al.*, Nucl. Phys. **B182**, 269 (1981).

¹⁰T. Kitagaki *et al.*, Phys. Rev. D **26**, 1554 (1982).

¹¹J. Pernegr, in *Multiparticle Dynamics 1981*, proceedings of the XIIth International Symposium, Notre Dame, Indiana, edited by W. D. Shephard and V. P. Kenney (World Scientific, Singapore, 1982), p. 119.

¹²D. Brick *et al.*, Z. Phys. C **19**, 1 (1983).

¹³M. Saleem *et al.*, Prog. Theor. Phys. **71**, 659 (1984).

¹⁴G. Bellini *et al.*, Nucl. Phys. **B199**, 1 (1982).

¹⁵S. A. Azimov *et al.*, Yad. Fiz. **35**, 950 (1982) [Sov. J. Nucl. Phys. **35**, 552 (1982)].

¹⁶M. Zielinski *et al.*, Z. Phys. C **16**, 197 (1983).

¹⁷M. Zielinski *et al.*, Phys. Rev. D **30**, 1855 (1984).

¹⁸J. Poirier, in *Multiparticle Dynamics 1981* (Ref. 11), p. 153; S. Mikocki *et al.*, Phys. Rev. D **34**, 42 (1986).

¹⁹T. Y. Chen *et al.*, Phys. Rev. D **28**, 2304 (1983).

²⁰C. C. Chang *et al.*, Phys. Rev. D **29**, 1888 (1984).

²¹J. W. Lamsa *et al.*, Phys. Rev. D **18**, 3933 (1978).

²²H. D. I. Abarbanel, Rev. Mod. Phys. **48**, 435 (1976).

²³P. Bosetti *et al.*, Nucl. Phys. **B101**, 304 (1975).

²⁴Particle Data Group, M. Aguilar-Benitez *et al.*, Phys. Lett. **170B**, 1 (1986).

²⁵C. Baltay *et al.*, Phys. Rev. D **17**, 62 (1978).